ACS OMEGA

http://pubs.acs.org/journal/acsodf

Article

Click Chemistry Actuated Exponential Amplification Reaction Assisted CRISPR−Cas12a for the Electrochemical Detection of MicroRNAs

Hongguo Wei, Shengjun Bu, Ze Wang, Hongyu Zhou, Xue Li, Jiaqi Wei, Xiuxia He,* and Jiayu Wan*

Cite This: *ACS Omega* 2022, 7, 35515−35522

Read Online

ACCESS | Metrics & More | Article Recommendations

ABSTRACT: MicroRNAs (miRNAs) play a very important role in biological processes and are used as biomarkers for the detection of a variety of diseases, including neurodegenerative diseases, chronic cardiovascular diseases, and cancers. A sensitive point-of-care (POC) method is crucial for detecting miRNAs. Herein, CRISPR−Cas12a combined with the click chemistry actuated exponential amplification reaction was introduced into an electrochemical biosensor for detecting miRNA-21. The target miRNA-21 initiated the click chemistry−exponential amplification reaction in the electrochemical biosensor to produce numerous nucleic acid fragments, which could stimulate the trans-cleavage ability of CRISPR−Cas12a to cleave hairpin DNA electrochemical reporters immobilized on the electrode surface. Under optimal conditions, the minimum detection limit for this electrochemical biosensor was as low as 1 fM. Thus, the proposed electrochemical biosensor allows sensitive and efficient miRNA detection and could be a potential analysis tool for POC test and field molecular diagnostics.

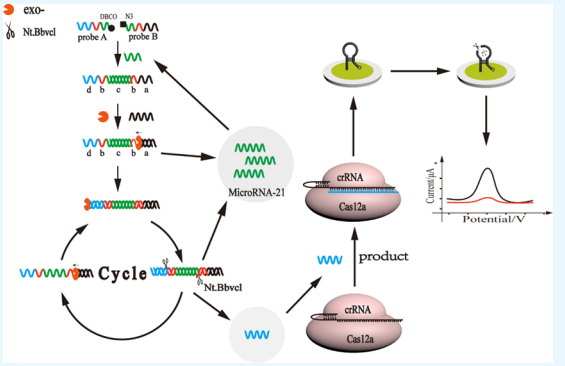

1. INTRODUCTION

Nucleic acid detection is a commonly used, efficient, and specific detection method, which plays a vital and significant role in rapid disease diagnosis, food safety, and environmental contamination detection.[1] A sensitive POC[2] meets the requirements of practical applications owing to its short time, cost-effectiveness, sample procedures, and high sensitivity. Therefore, the establishment of a POC method for nucleic acids detection is important for environmental contamination monitoring, food safety, and disease diagnosis.[3] In addition, the nucleic acid-based isothermal amplification strategies have become powerful tools in biosensing. Thus, their significance and development should be researched.[4]

Recently, the CRISPR−Cas12a system has attracted considerable attention of many scholars in the field of nucleic acid detection owing to the collateral cleavage activity of activated Cas12a to indiscriminately degrade any non-target single-stranded DNA reporter with hundreds of thousands of turnovers per minute.[5] The efficient collateral cleavage activity enables Cas12a protein to exhibit signal output, amplification, and reporting capabilities.[6] So far, the development of Cas12a-based diagnostic methods for the detection of DNA and RNA fragments with good practicality and sensitivity has revolutionized the field of molecular diagnosis to a certain extent[7,8] Dai et al. developed a universal electrochemical biosensor to detect viral nucleic acids based on the trans-cleavage activity of CRISPR−Cas12a.[9] Zhang et al. established a strategy of ultrasensitive miRNA detection based on CRISPR−Cas12a enhanced rolling circle amplification.[10] Gong et al. proposed a duplex-specific nuclease-assisted CRISPR−Cas12a strategy to detect microRNA (miRNA) with a personal glucose meter.[11]

miRNAs,[12] a class of small single-stranded RNAs composed of about 22 nucleotides, play important regulatory roles in a variety of biological processes by participating in the control of post-transcriptional gene expression,[13,14] including cell development, differentiation, immune response, and tumorigenesis, and have become biomarkers for many tumors in molecular diagnostics.[15] Currently, a few Cas12a-based assays for miRNA detection have been designed. For instance, Wang et al. described a Cas12a-derived miRNA sensing technology based on rolling circle transcription;[16] Sun et al. developed a Cas12a-mediated signal platform for the sensitive and specific detection of miRNA by coupling ligase-aided probe ligation, DNAzyme, and RNA polymerase-assisted amplification;[17] and Chen et al. established an ultrasensitive detection strategy for

Received: March 29, 2022
Accepted: May 16, 2022
Published: September 26, 2022

Scheme 1. Schematic Diagram of CRISPR−Cas12a-Mediated Electrochemical Detection of miRNA

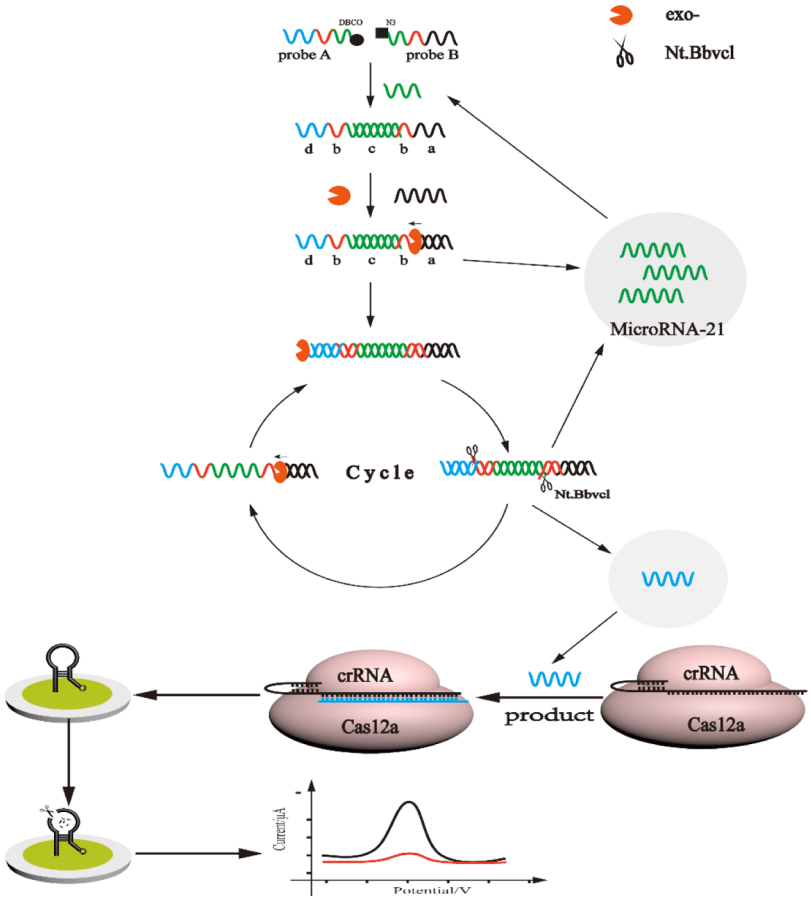

miR-21 based on mediated multistage displacement amplification and trans-cleavage activity of CRISPR/Cpf.[18] All these methods require some nucleic acid amplification techniques, such as rolling circle transcription, catalytic hairpin assembly, and so forth, to improve the Cas12a platform for detecting miRNA. Exponential amplification reaction (EXPAR), with the catalytic activity of DNA polymerase and endonuclease, can achieve rapid cycle amplification of a large number of short nucleic acid fragments and has received widespread attention because of its simplicity and sensitivity. In a standard EXPAR, short DNA primer hybridizes with the template strand and copies along the template chain with the help of DNA polymerase, and performs continuous displacement activities with the help of nicking endonuclease.[19] The nicking endonuclease recognizes specific sequences in the extended double chain, causing the nucleic acid chain to break and displacing the newly copied chain. The short strand is then hybridized with another template chain to start the next reaction cycle. In a previous study, by slightly modifying EXPAR for miRNA detection, a fluorescent biosensor had been constructed, with an improved target-induced chain amplification reaction.[20] Furthermore, Yang et al. successfully established a fluorescent biosensor to detect miRNA based on EXPAR-powered three-dimensional bipedal DNA walkers.[21] Besides, a sensitive fluorometric approach had been developed for assaying miRNA based on EXPAR combined with DNA-templated silver nanoclusters.[22]

In the present study, we established a highly sensitive electrochemical miRNA detection platform based on click chemistry actuated EXPAR and Cas12a (Scheme 1). The short miRNAs mediated the ligation of two oligonucleotide (ODN) probes into a long joint single-stranded DNA fragment, which was used as a template for EXPAR. Click chemistry, with advantages such as mild reaction conditions, positive selectivity, and high efficiency, has been widely researched since 2001. The enzyme-free click chemistry achieved high ligation efficiency between two ODNs modified with azide (N3) and Aza-dibenzocyclooctyne (Aza-DBCO) depending on the miRNA.[23,24] The resultant joint template, consisting of two nicking sites, in-between target miRNA binding site, primer binding site, and DNA fragment of Cas12a activator binding site, was extended to produce the final single-stranded DNA product (FP). The displaced target miRNA initiated[9] a two ODNs probe ligation reaction. The nicking endonuclease, Nt.BbvCI, recognized two cut points in the template copy chain and excised two strands (FP). One of the two DNA fragments presented the same sequence as that of the target miRNA, while the other activated Cas12a. The displaced identical DNA fragment of the target miRNA acted as a bridge to trigger the click reaction of the two ODN probes, further promoting the exponential generation of FPs. These extend, cut, extend, and replace reactions were repeated to produce a large number of short segments of DNA that could activate Cas12a. The DNA fragments activating Cas12a could turn on the trans-cleavage activity of Cas12a cleaving hairpin DNA electrochemical reporters immobilized on the electrode surface, thus changing the electrochemical signal.[25] To the best of our knowledge, the present study is the first to report on the application of electrochemical biosensor coupling Cas12a with click chemistry actuated EXPAR for miRNA

https://doi.org/10.1021/acsomega.2c01930
ACS Omega 2022, 7, 35515−35522

Table 1. DNA Fragments Used in This Study[a]

oligo names	sequences (5′−3′)
T7 promoter	GAAATTAATACGACTCACTATAGGG
crRNA-TP	TGCTTGTATTCCCAGCGTGCGCCATCTTAGTAGAAATTACCCTATAGTGAGTCGTATTA
MB-DNA	(SH-C6)-TCAGCGTTCCTTTACCATTTTTTTAACTTATTTGGTTTTTTTTTT-(MB)
Probe-A	GGCGCACGCTGGGAATACAAGCAGCTGAGGTCAACATCAGT-Aza-DBCO
Probe-B	N_3-CTGATAAGCTAGCTGAGGCCAAGGCCCAGCCCTCACACA
primer	TGTGTGAGGGCTGGGCCTTGG
miRNA21	UAGCUUAUCAGACUGAUGUUGA
miRNA21-1	UAGCUUA*A*CAGACUGAUGUUGA
miRNA21-2	UAGCUUA*A*CAGACUGAUGUUGC
miRNA21-3	UAGC*A*UA*A*CAGACUGAUGUUGC
miRNA21-4	UAGC*A*UAUC*A*UACUGAUGCUGC
miRNA141	UAACACUGUCUGGUAAAGAUGG

[a]The italic bases are the mutant bases.

quantification, providing valuable insights for the development of nucleic acid assays based on click chemistry actuated EXPAR and Cas12a.

2. EXPERIMENTAL SECTION

2.1. Chemicals and Instruments. Klenow fragment (3′-5′exo-) (5 U/μL) with enzyme liquid storage (100 mM KPO_4, 1 mM DTT, 0.1 mM EDTA, 50% glycerol; pH 7.4 at 25 °C) and 10× Klenow buffer (500 mM NaCl, 100 mM Tris−HCl, 100 mM $MgCl_2$, 10 mM DTT; pH 7.9 at 25 °C) were obtained from Sangon Biotech Co. Ltd (Shanghai, China). The dNTPs (25 mM) and 10× Tris−borate−EDTA (TBE) Premixed Powder were purchased from Sangon Biotech Co. Ltd. Nt.BbvCI (10 U/μL) with 10× CutSmart (100 mM $Mg(Ac)_2$, 200 mM Tris-Ac, 1000 μg/mL BSA, 500 mM KAc; pH 7.9 at 25 °C), HiScribe T7 Rapid and High Production RNA Synthesis Kit, MONARCH RNA Purification Kit, and LbaCas12a with 10× NEB buffer 2.1 (100 mM $MgCl_2$, 100 mM Tris−HCl, 1000 μg/mL BSA, 500 mM NaCl; pH 7.9 at 25 °C) were obtained from New England Biotechnology Co., Ltd. (MA, USA). 6-Mercapto-1-hexanol and Tris-(2-carboxyethyl)-phosphine hydrochloride (TCEP) were bought from Sigma-Aldrich (St. Louis, USA). All the DNA fragments used in this study were synthesized by Sangon Biotech Co. Ltd (Table 1). The specific sequence information about all the ODNs is presented in Table 1. Ultrapure water (18.2 MΩ cm) was provided by Milli-Q systems (Bedford, MA, USA), and all the nucleic acid chains were diluted with ultrapure water.

All the electrochemical signals were measured using a CHI 660E Electrochemical Workstation (Chen Hua Instrument, Shanghai, China). The electrode system included an Ag/AgCl electrode, platinum wire, and gold electrode as reference, auxiliary, and working electrodes, respectively. Gel electrophoresis was performed using an electrophoresis analyzer (Bio-Rad, USA) and visualized (Shenhua Technology Co. Ltd, China).

2.2. Synthesis of CRISPR RNA. A total of 2 μL of CRISPR RNA (crRNA) template and 2 μL of T7 promoter (100 μM) were mixed with 14 μL of RNase-free water, and the mixture was heated to 95 °C for 5 min. Then, the temperature of the mixture was slowly reduced to 25 °C for 20 min, and 10 μL of 100 mM dNTP buffer and 2 μL of T7 mix were added to the mixture. The single-stranded DNAs were degraded by DNase I, and the mixture was maintained at 37 °C for 15 min and supplemented with 45 μL of RNase-free water. Subsequently, the mixture was incubated at 37 °C for 16 h to obtain adequate mass of target crRNA. The crRNA transcription products were purified with miRcute miRNA Isolation Kit and centrifuged at 13,000 rpm for 1 min. Then, the products were washed thrice with washing buffer and stored in enzyme-free tubes. Finally, the concentration of the obtained crRNA was adjusted with NanoDrop 2000C and stored at −80 °C.

2.3. Electrode Treatment and Functionalization of Sensing Surface. First, the gold electrode was polished with aluminum powder (0.05%) to achieve mirror-like smoothness on the electrode surface. Next, an ultrasound was performed with deionized water to remove dust from the surface of the gold electrode. Then, the gold electrode was placed in a freshly prepared piranha solution (volume ratio: H_2SO_4/H_2O_2 = 3:1) for 30 min to corrode impurities, rinsed thoroughly with deionized water, and electrochemically evaluated in 0.5 M H_2SO_4 with a CV range from 0.2 to 1.4 V and a scan rate of 50 mV/s until a stable full CV peak was obtained. The electrochemical impedance spectroscopy (EIS) was performed with an amplitude of 5 mV and a frequency sweep range of 0.1−10^5 Hz. The differential pulse voltammetry (DPV) signals were recorded within the range from −0.15 to 0.4 V and scan rate of 50 mV in 20 mM PBS (2.5 mM $MgCl_2$, 50 mM NaCl; pH 7.4). For immobilization onto the gold electrode, DNA-MB was dissolved using 10 mM TCEP in 10 mM Tris−HCl buffer solution (containing 5 mM $MgCl_2$, 0.5 M NaCl; pH 7.4). Subsequently, 10 μL of DNA-MB were added onto the pretreated electrode surface and incubated at room temperature for 10 h in dark. Then, the electrode was rinsed with ultrapure water and 5 μL of 1 mM MCH solution were added onto the electrode for 60 min. Finally, the residue on the electrode surface was completely removed with ultrapure water, allowing the electrode to be used for subsequent operation.

2.4. Gel Electrophoresis. A 15% natural polyacrylamide gel was prepared to determine the ligation products of click chemistry. The electrophoresis was conducted in 1× TBE buffer (89 mM Tris-boric acid, 2 mM EDTA; pH 8.2−8.4 at 25 °C) at 180 V for 30 min. Subsequently, the gel was stained with 10× SYBR Green II and visualized using a gel image system.

2.5. Target miRNA Detection. Various concentrations of miRNA and ODNs containing probe A and probe B (each 1 μM), which were, respectively, modified using Aza-DBCO and N3, were maintained at 37 °C for 60 min. Then, 6 μL of the ligation product and 1 μL of 10 μM primer were mixed in 4 μL of 10× Klenow buffer and 10× CutSmart, and the mixture was

https://doi.org/10.1021/acsomega.2c01930
ACS Omega 2022, 7, 35515−35522

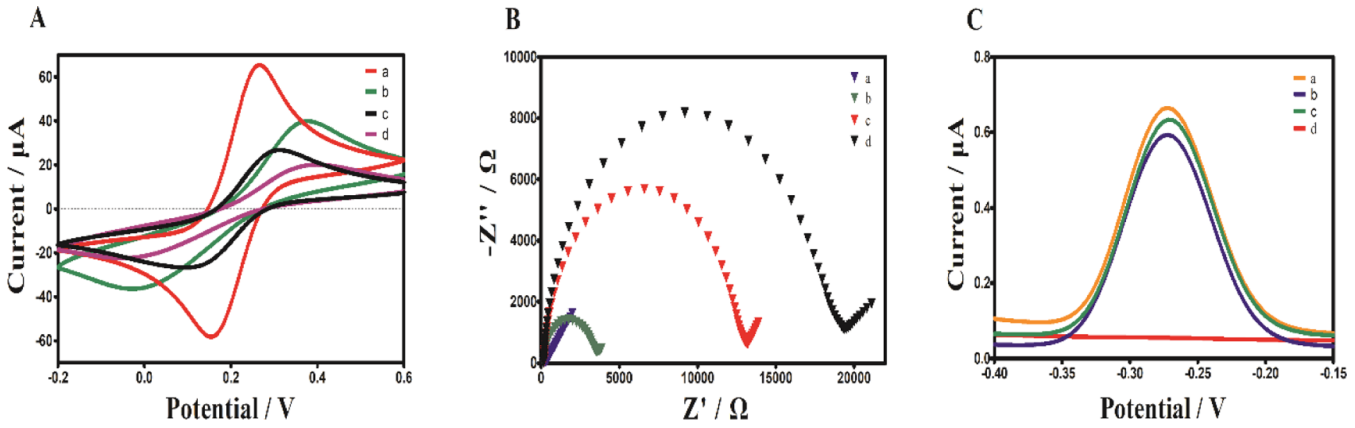

Figure 1. CV (A), EIS (B), and DPV (C) response of the developed biosensor (A) (a) bare electrode, (b) DNA-MB-MCH-Cas12a-modified electrode, (c) DNA-MB-modified electrode, and (d) DNA-MB-MCH-modified electrode; (B) (a) bare electrode, (b) DNA-MB-MCH-Cas12a-modified electrode, (c) DNA-MB-modified electrode, and (d) DNA-MB-MCH-MCH-modified electrode; and (C) (a) blank negative control; (b) DNA-MB-MCH-Cas12a without crRNA; (c) DNA-MB-MCH; and (d) DNA-MB-MCH-Cas12a.

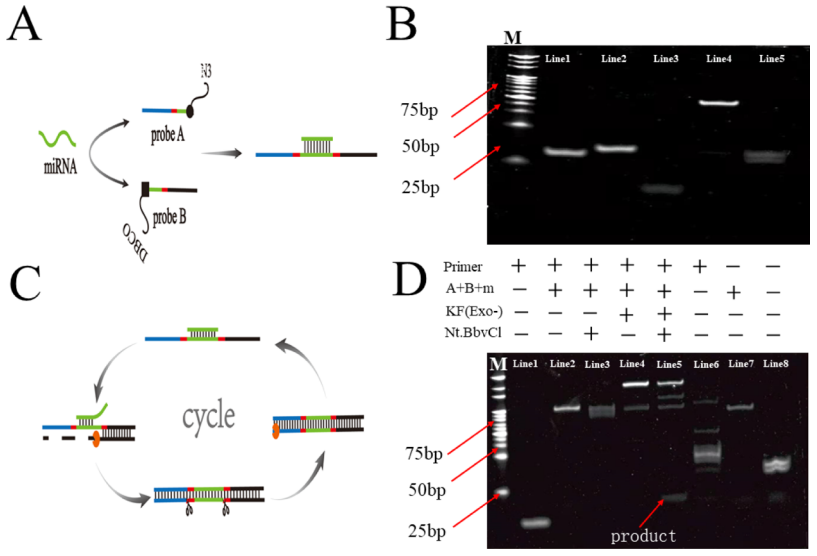

Figure 2. (A) Schematic representation of the mechanism of click reaction. (B) Gel electrophoresis to determine the ligation products of click chemistry. From left to right: lane 1, probe A; lane 2, probe B; lane 3, miRNA21; lane 4, probe A + probe B + miRNA21; and lane 5, probe A + probe B without miRNA21. (C) Schematic representation of the mechanism of the EXPAR reaction. (D) Lane 1, primer; lane 2, primer + click reaction product; lane 3, primer + click reaction product with Nt.BbvCl; lane 4, primer + click reaction product with KF(EXO-); lane 5, experimental (with miRNA21); lane 6, control groups (without miRNA21); lane 7, probe A + probe B + miRNA21; and lane 8, probe A + probe B without miRNA21. The first lane is the Marker.

heated to 95 °C for 5 min. Subsequently, the mixture was slowly cooled to 25 °C for more than 20 min, and 4 μL of 25 mM dNTPs, 0.5 μL of 5 U/μL Klenow fragment, and 0.5 μL of 10 U/μL. Nt.BbvCI was added to the mixture. The final volume of the mixture was made to 20 μL by adding ddH_2O. The reaction system was incubated at 37 °C for 80 min and then at 80 °C for 20 min to make the Klenow fragment and Nt.BbvCI lose their activity. Next, 7 μL of the product of the reaction, 4 μL of 0.3 μM LbCas12a, 1 μL of 4 μM crRNA, and 1 μL of RNase were added to the system, and finally, the mixture was dropped onto the gold electrode.

3. RESULTS AND DISCUSSION

3.1. Design of the Proposed Method. Scheme 1 depicts the detailed workflow of the CRISPR/Cas sensor by using miRNA21 as a proof-of-concept target. miRNA21 could promote the click chemical ligation reaction between ODNs through complementary hybridization. In the presence of miRNA21, though the click chemistry reaction to produce the template which were as the EXPAR reaction template, the whole amplification process of click chemistry-EXPAR was similar to a net with multiple endless cycles which can amplify lots of DNA fragments that are able to turn on the trans-cleavage activity of CRISPR/Cas12a. Each miRNA21 acted as a bridge linking ODNs to produce a 3′-5′exo-replication template. The template bound to primers to initiate DNA polymerization in the presence of dNTPs. Subsequently, a double-stranded DNA was generated with two recognition sites that were identified by the added Nt.BbvCI, and the phosphodiester bond of the double-stranded DNA was excised producing 3′-OH ends. EXPAR generated a large number of product fragments and initiated the CRISPR−Cas12a system, as well as generated a nucleic acid sequence that can bridge the click chemical ligation reaction and ensue the cycle 2 reaction.

https://doi.org/10.1021/acsomega.2c01930
ACS Omega 2022, 7, 35515−35522

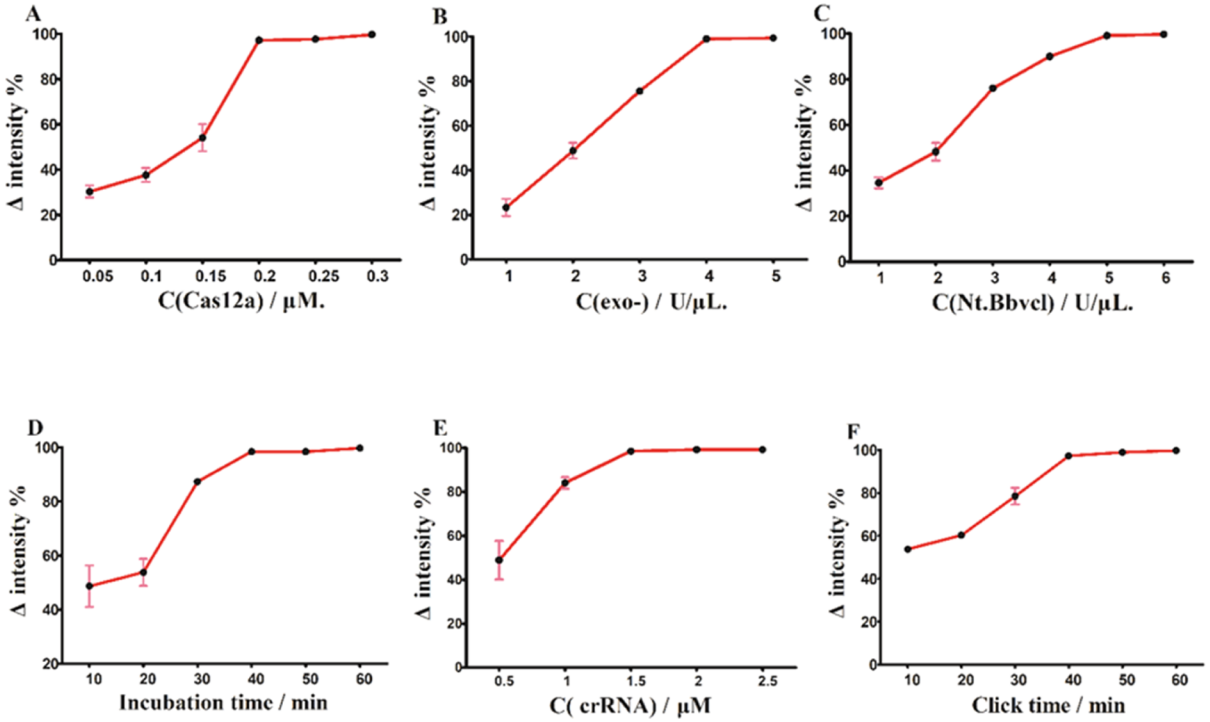

Figure 3. Optimization of the experimental conditions. (A) Cas12a concentration; (B) dosage of Klenow fragment; (C) Nt.BbvCI concentration; (D) EXPAR reaction time; (E) CrRNA concentration; and (F) click chemistry reaction time.

3.2. Electrochemical Characterization of the Developed Biosensor. Owing to the efficient electron transfer capability of the electrochemical biosensor surface, a pair of clear REDOX peaks could be observed for the pretreated bare gold electrode. However, after DNA-MB was fixed on the surface of the gold electrode, electron transfer was significantly inhibited and the REDOX peak was notably reduced. Moreover, the addition of MCH blocked the surplus active sites and further reduced the CV signal. In contrast, following cleavage by CRISPR−Cas12a, the modified MB-DNA was detached from the electrode and the electroactive site was again exposed, resulting in an increase in the REDOX peak (Figure 1A). Figure 2 shows the outcomes of EIS performed in $[Fe(CN)_6]^{3-/4-}$ solution. When compared with bare electrodes, the diameter of the semicircle increased with the stepwise modification of the resistance of DNA-MB. Following surface blocking with MCH, the resistance of DNA-MB-MCH-modified electrodes further increased owing to the increase in the electron transfer resistance. As expected, after being cleaved by CRISPR−Cas12a, the resistance response curve of the DNA-MB-MCH-modified electrodes was reduced. These phenomena indicated successful preparation of the CRISPR−Cas12a biosensor (Figure 1B) and showed the feasibility of using the proposed sensor under different conditions. As a signal output label, MB caused an intense DPV response and produced strong peak current, which was owing to the requirement of crRNA binding to boot the system; in contrast, in the absence of crRNA, the signal was essentially unchanged. Furthermore, the absence of Cas12a had a negligible effect on the DPV signal (Figure 1C).

3.3. Gel Electrophoresis. We employed 15% native polyacrylamide gel electrophoresis to examine whether miRNA can be ligated to probe A and probe B (click chemistry) and EXPAR (Figure 2). Figure 2A presents a schematic of click chemistry. As shown in Figure 2B, lanes 1−3 represent probe A, probe B, and miRNA21, respectively; lane 4 denotes ligation of probe A, probe B, and miRNA21; and lane 5 reveals probe A and probe B without miRNA21. It can be observed from the figure that probe A and probe B are ligated together in the presence of miRNA and the combination efficiency is good. Figure 2C illustrates the EXPAR reflection process. As can be seen in Figure 2D, lane 1 represents primer; lane 2 contains probe A, probe B, miRNA21, and primer; lane 3 contains probe A, probe B, miRNA21, primer, Nt.BbvCI, and without Klenow fragment [we observed that the long strand (probe A + probe B) did not replicate]; and lane 4 represents probe A, probe B, miRNA21, primer, Klenow fragment, and without Nt.BbvCI. In lane 4, only a bright band was observed and without product, whereas lanes 5 and 6 reflected the gel bands of the experimental (with miRNA21) and control (without miRNA21) groups, respectively. The product can be detected in the experimental band.

3.4. Optimization of the Experimental Conditions. To accomplish better detection performance of the developed electrochemical biosensor, six parameters that affect the detection reaction were optimized to different degrees: (A) CRISPR-Cas12a concentration; (B) Klenow fragment (3′-5′exo-) concentration; (C) Nt.BbvCI concentration; (D) EXPAR reaction time; (E) crRNA concentration; and (F) click chemistry reaction time. As illustrated in Figure 3A, the change in signal intensity (ΔI %) was calculated as follows: ΔI %= (background signal − target signal)/background signal) × 100%. It can be observed from Figure 3A that the shearing efficiency of CRISPR−Cas12a increased with the increase in concentration of CRISPR−Cas12a. Accordingly, to save cost, we selected 0.2 μM as the optimal CRISPR−Cas12a concentration. The concentrations of the Klenow fragment and Nt.BbvCI were found to be the key factors that affect the efficiency of EXPAR. The highest shearing efficiency of CRISPR−Cas12a was noted when 4 U/μL Klenow fragment

https://doi.org/10.1021/acsomega.2c01930
ACS Omega 2022, 7, 35515−35522

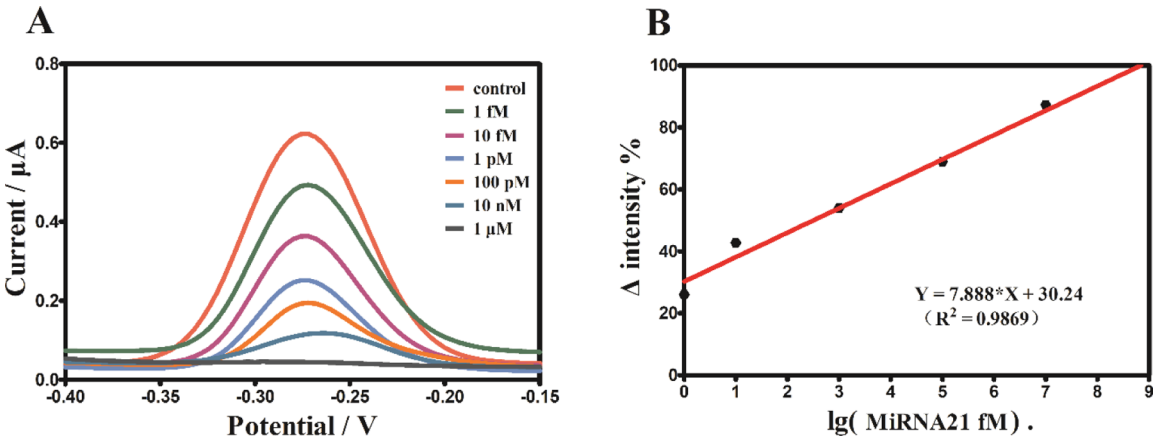

Figure 4. Quantification of target miRNA21 using the proposed method. (A) Sensitivity of the developed electrochemical sensor to detect miRNA21. (B) Calibration plot of the peak current intensity of DPV vs lg *c*. Each miRNA21 concentration was assayed thrice.

was employed. With regard to Nt.BbvCI concentration, ΔI % gradually improved with the increase in concentration of Nt.BbvCI, and reached its peak at 4 U/μL Nt.BbvCI (Figure 3B). Hence, 5 U/μL Nt.BbvCI was chosen as the optimal concentration in the present study (Figure 3C). When the EXPAR reaction time was increased from 20 to 40 min, the shearing efficiency of CRISPR−Cas12a rapidly increased; however, with further increases in the reaction time, the shearing efficiency remained relatively stable. Therefore, 40 min was selected as the optimal EXPAR reaction time (Figure 3D). Investigation of the effects of six different crRNA concentrations (50, 100, 150, 200, and 250 nM) revealed that the shearing efficiency of the CRISPR−Cas12a system remained stable with the increase in crRNA concentration (Figure 3E). Furthermore, miRNA, probe A, and probe B also affected ΔI % through the click chemistry reaction time, and ΔI % increased with the increase in click chemistry reaction time (Figure 3F).

3.5. Quantification of Target miRNA21. To examine the ability of the proposed method to detect miRNA21 under optimal experimental conditions, a series of solutions containing different miRNA21 concentrations were investigated. The peak current induced by MB changed with the increase in miRNA21 concentration. The ΔI % gradually decreased with the decrease in concentration of miRNA21 (10^0, 10^1, 10^3, 10^5, 10^7, 10^9, and control fM), indicating a sensitive response correlation between miRNA21 concentration and DPV signal (Figure 4A), and the linear equation can be given as follows: ΔI % = 7.888 × X + 30.24 (R^2 = 0.9869) with a detection limit of 1 fM (Figure 4B). When compared with some previously reported miRNA detection methods (Table 2) and combined CRISPR systems (Table 3), these results demonstrated that the developed electrochemical sensor had good sensitivity for the detection of miRNA.

3.6. Specificity. To evaluate the selectivity and specificity of the developed electrochemical biosensor, different miRNAs with varying degrees of mutation, including miRNA21-1 (1 μM), miRNA21-2 (1 μM), miRNA21-3 (1 μM), miRNA21-4 (1 μM), and miRNA141 (1 μM), were used under the same reaction conditions. As shown in Figure 5, miRNA21 presented a strong reaction throughout the experiment, with the decrease in DPV signal and increase in ΔI%. In contrast, miRNA141, miRNA21-1, miRNA21-2, miRNA21-3, and miRNA21-4 showed no significant changes in DPV signals,

Table 2. Comparisons Among Different Methods for miRNA Detection

type of biosensor	detection range	detection limit	ref
fluorescent detection	100 pM to 250 nM	9.01 pM	26
colorimetric detection	50 pM to 10 nM	27.1 pM	27
fluorescent detection	0.5−50 nM	72 pM	28
electrochemical detection	30 pM to 7 nM	11 pM	29
fluorescent detection	0.8 nM to 60 nM	0.8 nM	30
electrochemical detection	1 μM to 1 fM	1 fM	this work

and Cas12a did not produce any response, which were almost similar to that noted in the blank control. These results indicated that the developed electrochemical biosensor was highly specific and effective.

3.7. Recovery Test. The recovery test was performed to confirm the practicability of the developed biosensor platform, as well as its application potential and reliability for nucleic acid detection. In brief, different concentrations of miRNA-21 (10^7, 10^5, and 10^3 fM) were spiked into 10× diluted real biological serum samples and examined using the developed electrochemical biosensor. As shown in Table 4, the recoveries were 98.2, 97.3, and 100.9% for samples spiked with 10^7, 10^5, and 10^3 fM miRNA21, respectively, demonstrating that the developed biosensor could effectively detect miRNA21 in complex environments and different biological samples.

4. CONCLUSIONS

In this study, we developed a click chemistry-EXPAR-based CRISPR−Cas12a electrochemical biosensor for the sensitive detection of miRNA. The biosensor combined self-signal amplification of the CRISPR−Cas12a system with click chemistry-EXPAR-mediated signal conversion, achieving multiple cycles of miRNA amplification detection, with high efficiency and sensitivity. Given the immobilization ability and extendibility of click chemistry-EXPAR, the developed biosensor could also be applied to different miRNA targets without altering the CRISPR−Cas12a components and only requiring modification in a portion of nucleic acid sequence of the two nucleic acid probes for miRNA. The versatility of the developed electrochemical biosensor was confirmed by using real serum samples spiked with different concentrations of

https://doi.org/10.1021/acsomega.2c01930
ACS Omega 2022, 7, 35515−35522

Table 3. Comparisons Among Different Combined CRISPR Systems

type of biosensor	element	advantage	disadvantage	detection range	detection limit	ref
E-CRIPSR (based electrochemical biosensor)	viral nucleic acids	sample and convenient	low sensitivity and high false positive	1 nM to 50 nM	0.2 nM	30
CRISPR/Cas12a electrochemical detection	DNA	rapid test	low sensitivity	50 pM to 100 nM	30 pM	31
CRISPR/Cas13a-triggered RCA-DNAzyme	miR-10b	high sensitivity	complex operation	100 aM to 100 pM	1 fM	32
CRISPR−Cas13-fluorescent detection	Nucleic Acid	rapid test high sensitivity	complex operation	aM	2 aM	33
CRISPR/Cas13a powered portable electrochemiluminescence chip	miR-17	strong innovative	complicated operation	100×10^{-12} M to 1×10^{-15} M	1×10^{-15} M	34

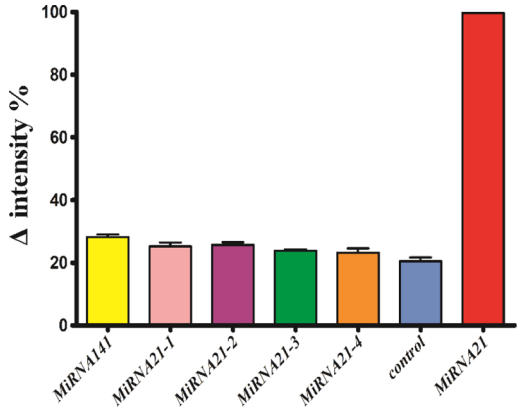

Figure 5. Specificity of the developed electrochemical biosensor (miRNA concentration: 1 μM). Error bar is the standard deviation of at least triplicate measurements.

Table 4. Detection of miRNAs in Real Serum Samples Using the Developed Biosensor

original value (fM)	added (fM)	detected (fM)	recovery ± RSD (%)
0	1×10^7	0.98×10^7	98.2 ± 7.8
0	1×10^5	0.97×10^5	97.3 ± 5.7
0	1×10^3	1.01×10^3	100.9 ± 2.6

miRNA21. Thus, the present study expands the application of the biosensor to miRNA detection, and the developed electrochemical biosensor could be a valuable tool for clinical prediction and molecular diagnosis.

AUTHOR INFORMATION

Corresponding Authors

Xiuxia He − *School of Life Science and Technology, Changchun University of Science and Technology, Changchun 130022, China*; Email: wanjiayu@hotmail.com

Jiayu Wan − *Institute of Military Veterinary Medicine, Academy of Military Medical Sciences, Changchun 130122, China*; orcid.org/0000-0002-1358-4143; Email: hexx@cust.edu.cn

Authors

Hongguo Wei − *School of Life Science and Technology, Changchun University of Science and Technology, Changchun 130022, China; Institute of Military Veterinary Medicine, Academy of Military Medical Sciences, Changchun 130122, China*

Shengjun Bu − *Institute of Military Veterinary Medicine, Academy of Military Medical Sciences, Changchun 130122, China*

Ze Wang − *Institute of Military Veterinary Medicine, Academy of Military Medical Sciences, Changchun 130122, China*

Hongyu Zhou − *Institute of Military Veterinary Medicine, Academy of Military Medical Sciences, Changchun 130122, China*

Xue Li − *Institute of Military Veterinary Medicine, Academy of Military Medical Sciences, Changchun 130122, China*

Jiaqi Wei − *Institute of Military Veterinary Medicine, Academy of Military Medical Sciences, Changchun 130122, China*

Complete contact information is available at: https://pubs.acs.org/10.1021/acsomega.2c01930

Notes

The authors declare no competing financial interest.

ACKNOWLEDGMENTS

This work was financially supported by the Science and Technology Development Project of Jilin Province (20150101105JC).

REFERENCES

(1) Xiong, Y.; Zhang, J.; Yang, Z.; Mou, Q.; Ma, Y.; Xiong, Y.; Lu, Y. Functional DNA Regulated CRISPR-Cas12a Sensors for Point-of-Care Diagnostics of Non-Nucleic-Acid Targets. *J. Am. Chem. Soc.* **2020**, *142*, 207−213.

(2) Yu, Z.; Gong, H.; Xu, J.; Li, Y.; Zeng, Y.; Liu, X.; Tang, D. Exploiting Photoelectric Activities and Piezoelectric Properties of NaNbO3 Semiconductors for Point-of-Care Immunoassay. *Anal. Chem.* **2022**, *94*, 3418−3426.

(3) Wang, Y.; Yu, L.; Kong, X.; Sun, L. Application of nanodiagnostics in point-of-care tests for infectious diseases. *Int. J. Nanomed.* **2017**, *12*, 4789−4803.

(4) Yu, Z.; Cai, G.; Tong, P.; Tang, D. Saw-Toothed Microstructure-Based Flexible Pressure Sensor as the Signal Readout for Point-of-Care Immunoassay. *ACS Sens.* **2019**, *4*, 2272−2276.

(5) Li, Y.; Li, S.; Wang, J.; Liu, G. CRISPR/Cas Systems towards Next-Generation Biosensing. *Trends Biotechnol.* **2019**, *37*, 730−743.

(6) Zhang, L.; Jiang, H.; Zhu, Z.; Liu, J.; Li, B. Integrating CRISPR/Cas within isothermal amplification for point-of-Care Assay of nucleic acid. *Talanta* **2022**, *243*, 123388.

(7) Peng, S.; Tan, Z.; Chen, S.; Lei, C.; Nie, Z. Integrating CRISPR-Cas12a with a DNA circuit as a generic sensing platform for amplified detection of microRNA. *Chem. Sci.* **2020**, *11*, 7362−7368.

(8) Wei, J.; Gong, X.; Wang, Q.; Pan, M.; Liu, X.; Liu, J.; Xia, F.; Wang, F. Construction of an autonomously concatenated hybridization chain reaction for signal amplification and intracellular imaging. *Chem. Sci.* **2018**, *9*, 52−61.

(9) Dai, Y.; Somoza, R. A.; Wang, L.; Welter, J. F.; Li, Y.; Caplan, A. I.; Liu, C. C. Exploring the Trans-Cleavage Activity of CRISPR-Cas12a (cpf1) for the Development of a Universal Electrochemical Biosensor. *Angew. Chem., Int. Ed. Engl.* **2019**, *58*, 17399−17405.

(10) Zhang, G.; Zhang, L.; Tong, J.; Zhao, X.; Ren, J. CRISPR-Cas12a enhanced rolling circle amplification method for ultrasensitive miRNA detection. *Microchem. J.* **2020**, *158*, 105239.

(11) Gong, S.; Li, J.; Pan, W.; Li, N.; Tang, B. Duplex-Specific Nuclease-Assisted CRISPR-Cas12a Strategy for MicroRNA Detection

https://doi.org/10.1021/acsomega.2c01930
ACS Omega 2022, 7, 35515−35522

Using a Personal Glucose Meter. *Anal. Chem.* **2021**, *93*, 10719−10726.
(12) Huang, S.; He, X. microRNAs: tiny RNA molecules, huge driving forces to move the cell. *Protein Cell* **2010**, *1*, 916−926.
(13) Jiang, L.; Yang, Y.; Lin, Y.; Chen, Z.; Xing, C.; Lu, C.; Yang, H.; Zhang, S. An electrochemical sensor based on enzyme-free recycling amplification for sensitive and specific detection of miRNAs from cancer cells. *Analyst* **2020**, *145*, 3353−3358.
(14) Pothipor, C.; Jakmunee, J.; Bamrungsap, S.; Ounnunkad, K. An electrochemical biosensor for simultaneous detection of breast cancer clinically related microRNAs based on a gold nanoparticles/graphene quantum dots/graphene oxide film. *Analyst* **2021**, *146*, 4000−4009.
(15) Zheng, W.; Yao, L.; Teng, J.; Yan, C.; Qin, P.; Liu, G.; Chen, W. Lateral flow test for visual detection of multiple MicroRNAs. *Sens. Actuators, B* **2018**, *264*, 320−326.
(16) Wang, G.; Tian, W.; Liu, X.; Ren, W.; Liu, C. New CRISPR-Derived microRNA Sensing Mechanism Based on Cas12a Self-Powered and Rolling Circle Transcription-Unleashed Real-Time crRNA Recruiting. *Anal. Chem.* **2020**, *92*, 6702−6708.
(17) Sun, H.-H.; He, F.; Wang, T.; Yin, B.-C.; Ye, B.-C. A Cas12a-mediated cascade amplification method for microRNA detection. *Analyst* **2020**, *145*, 5547−5552.
(18) Chen, X.; Deng, Y.; Cao, G.; Xiong, Y.; Huo, D.; Hou, C. Ultrasensitive MicroRNA-21 detection based on multiple cascaded strand displacement amplification and CRISPR/Cpf1 (MC-SDA/CRISPR/Cpf1). *Chem. Commun.* **2021**, *57*, 6129−6132.
(19) Zhang, Y.-P.; Cui, Y.-X.; Li, X.-Y.; Du, Y.-C.; Tang, A.-N.; Kong, D.-M. A modified exponential amplification reaction (EXPAR) with an improved signal-to-noise ratio for ultrasensitive detection of polynucleotide kinase. *Chem. Commun.* **2019**, *55*, 7611−7614.
(20) Huang, M.; Zhou, X.; Wang, H.; Xing, D. Clustered Regularly Interspaced Short Palindromic Repeats/Cas9 Triggered Isothermal Amplification for Site-Specific Nucleic Acid Detection. *Anal. Chem.* **2018**, *90*, 2193−2200.
(21) Yang, X.; Tang, Y.; Mason, S. D.; Chen, J.; Li, F. Enzyme-Powered Three-Dimensional DNA Nanomachine for DNA Walking, Payload Release, and Biosensing. *ACS Nano* **2016**, *10*, 2324−2330.
(22) Reid, M. S.; Le, X. C.; Zhang, H. Exponential Isothermal Amplification of Nucleic Acids and Assays for Proteins, Cells, Small Molecules, and Enzyme Activities: An EXPAR Example. *Angew. Chem., Int. Ed. Engl.* **2018**, *57*, 11856−11866.
(23) Heuer-Jungemann, A.; Kirkwood, R.; El-Sagheer, A. H.; Brown, T.; Kanaras, A. G. Copper-free click chemistry as an emerging tool for the programmed ligation of DNA-functionalised gold nanoparticles. *Nanoscale* **2013**, *5*, 7209−7212.
(24) Oishi, M. Enzyme-free and isothermal detection of microRNA based on click-chemical ligation-assisted hybridization coupled with hybridization chain reaction signal amplification. *Anal. Bioanal. Chem.* **2015**, *407*, 4165−4172.
(25) Yuan, H.; Liu, Z.; Xu, G.; Zhou, B.; Wu, S.; Dumcenco, D.; Yan, K.; Zhang, Y.; Mo, S.-K.; Dudin, P.; Kandyba, V.; Yablonskikh, M.; Barinov, A.; Shen, Z.; Zhang, S.; Huang, Y.; Xu, X.; Hussain, Z.; Hwang, H. Y.; Cui, Y.; Chen, Y. Evolution of the Valley Position in Bulk Transition-Metal Chalcogenides and Their Monolayer Limit. *Nano Lett.* **2016**, *16*, 4738−4745.
(26) Pu, J.; Liu, M.; Li, H.; Liao, Z.; Zhao, W.; Wang, S.; Zhang, Y.; Yu, R. One-step enzyme-free detection of the miRNA let-7a via twin-stage signal amplification. *Talanta* **2021**, *230*, 122158.
(27) Chen, W.; Zhang, X.; Li, J.; Chen, L.; Wang, N.; Yu, S.; Li, G.; Xiong, L.; Ju, H. Colorimetric Detection of Nucleic Acids through Triplex-Hybridization Chain Reaction and DNA-Controlled Growth of Platinum Nanoparticles on Graphene Oxide. *Anal. Chem.* **2020**, *92*, 2714−2721.
(28) Liu, Y.; Shen, T.; Li, J.; Gong, H.; Chen, C.; Chen, X.; Cai, C. Ratiometric Fluorescence Sensor for the MicroRNA Determination by Catalyzed Hairpin Assembly. *ACS Sens.* **2017**, *2*, 1430−1434.
(29) Liang, M.; Pan, M.; Hu, J.; Wang, F.; Liu, X. Electrochemical Biosensor for MicroRNA Detection Based on Cascade Hybridization Chain Reaction. *ChemElectroChem* **2018**, *5*, 1380−1386.
(30) Song, C.; Wang, G.-Y.; Kong, D.-M. A facile fluorescence method for versatile biomolecular detection based on pristine alpha-Fe(2)O(3) nanoparticle-induced fluorescence quenching. *Biosens. Bioelectron.* **2015**, *68*, 239−244.
(31) Zhang, D.; Yan, Y.; Que, H.; Yang, T.; Cheng, X.; Ding, S.; Zhang, X.; Cheng, W. CRISPR/Cas12a-Mediated Interfacial Cleaving of Hairpin DNA Reporter for Electrochemical Nucleic Acid Sensing. *ACS Sens.* **2020**, *5*, 557−562.
(32) Zhou, T.; Huang, M.; Lin, J.; Huang, R.; Xing, D. High-Fidelity CRISPR/Cas13a trans-Cleavage-Triggered Rolling Circle Amplified DNAzyme for Visual Profiling of MicroRNA. *Anal. Chem.* **2021**, *93*, 2038−2044.
(33) Abudayyeh, O. O.; Gootenberg, J. S.; Kellner, M. J.; Zhang, F. Nucleic Acid Detection of Plant Genes Using CRISPR-Cas13. *CRISPR J.* **2019**, *2*, 165−171.
(34) Zhou, T.; Huang, R.; Huang, M.; Shen, J.; Shan, Y.; Xing, D. CRISPR/Cas13a Powered Portable Electrochemiluminescence Chip for Ultrasensitive and Specific MiRNA Detection. *Adv. Sci.* **2020**, *7*, 1903661.

https://doi.org/10.1021/acsomega.2c01930
ACS Omega 2022, 7, 35515−35522